Quaternary Research 73 (2010) 573–582

Contents lists available at ScienceDirect

Quaternary Research

journal homepage: www.elsevier.com/locate/yqres

Latitudinal and downcore (0–750 ka) changes in *n*-alkane chain lengths in the eastern equatorial Pacific

Keiji Horikawa [a,b,c,*], Masafumi Murayama [b], Masao Minagawa [a], Yoshihisa Kato [d], Takuya Sagawa [b]

[a] Graduate School of Environmental Science, Hokkaido University, Sapporo 060-0810, Japan
[b] Center for Advanced Marine Core Research, Kochi University, B200 Monobe, Nankoku 783-8502, Japan
[c] Graduate School of Environmental Studies, Nagoya University, Furo-cho, Chikusa-ku, Nagoya 464-8601, Japan
[d] School of Marine Science and Technology, Tokai University, Shizuoka 424-8610, Japan

ARTICLE INFO

Article history:
Received 21 June 2009
Available online 12 February 2010

Keywords:
n-alkane
Vegetation change
MIS 13
Eastern equatorial Pacific
Mid-Pleistocene Transition

ABSTRACT

The *n*-alkane $C_{31}/(C_{29}+C_{31})$ ratios from surface sediments in the eastern equatorial Pacific (EEP) exhibit higher values to the north and lower values to the south across the southern edge (2–4°N) of the Intertropical Convergence Zone (ITCZ). Since plants tend to synthesize longer chain length *n*-alkanes in response to elevated temperature and/or aridity, the higher $C_{31}/(C_{29}+C_{31})$ ratios at northern sites suggest a higher contribution of vegetation under hot and/or dry conditions. This is consistent with the observation that northern sites receive higher levels of plant waxes transported by northeasterly trade winds from northern South America, where hot and dry conditions prevail. Furthermore, from a sediment core covering the past 750 ka (core HY04; 4°N, 95°W) we found that $C_{31}/(C_{29}+C_{31})$ ratios exhibit a long-term decrease from MIS (marine oxygen isotope stage) 17 to 13. During this period, the zonal SST (sea-surface temperature) gradient in the equatorial Pacific increased, suggesting an increase in Walker circulation. Such intensified Walker circulation may have enhanced moisture advection from the equatorial Atlantic warm pool to the adjacent northern South America, causing arid regions in northern South America to contract, which may explain long-term decrease in *n*-alkane chain lengths.

Introduction

The dominant periodicity of the change in global ice volume was altered from obliquity cycles to large-amplitude eccentricity cycles during the Mid-Pleistocene Transition (MPT; 1.25–0.6 Ma) (e.g., Mudelsee and Schulz, 1997; Medina-Elizalde and Lea, 2005). At the same time, the polar ice sheet gradually expanded, and atmospheric CO_2 concentration increased about 25 p.p.m.v. from 0.8 to 0.4 Ma (Lüthi et al., 2008). Further, the mean ocean $\delta^{13}C$ value exhibited a long-term increase by 0.3–0.4‰ during the same period (e.g., Raymo et al., 1997; Mohtadi et al., 2006). These records strongly indicate that a substantial perturbation in climate systems occurred during and just after the MPT and that the climate system adjusted to new boundary conditions with amplification of the 100-kyr cycle. Yet, how terrestrial systems responded to the climate perturbation during the Mid-Pleistocene is poorly understood given the scarcity of long-term Pleistocene records of continental climate and vegetation. These records are important to understanding climate perturbations during the Mid-Pleistocene because changes in ocean-atmosphere circulation have the potential to alter hydrological cycles on land, which may in turn affect climate through vegetation feedback mechanisms, such as albedo and biogeochemical cycling (CO_2 and CH_4) (e.g., Dupont et al., 2001; Schefuß et al., 2003a).

Long-chain, odd-numbered *n*-C_{25} to *n*-C_{33} alkanes are major lipid constituents of land plant epicuticular waxes (e.g., Eglinton and Hamilton, 1967). These plant waxes are easily removed from the leaf surface by rain or wind; sandblasting during dust storms is a significant factor (Conte and Weber, 2002). They are therefore common organic components of eolian dust and in marine sediments (e.g., Gagosian et al., 1987; Ohkouchi et al., 1997). Long-chain, odd-numbered *n*-alkanes are produced as moisture-regulating epicuticular leaf waxes (Tulloch, 1976), and longer chain length *n*-alkanes tend to be synthesized under water stress conditions in response to elevated temperatures and aridity (e.g., Dodd and Rafii, 2000). In fact, surface sediments and atmospheric dust samples collected off West Africa reveal changes in chain length distributions of *n*-alkanes in response to aridity in the source regions (Huang et al., 2000; Rommerskirchen et al., 2003; Schefuß et al., 2003b). Therefore, chain lengths are thought to have the potential to provide a first-order sign of temperature/aridity changes on adjacent lands in the past, as well as compound-specific $\delta^{13}C$ and δD of land plant-derived *n*-alkanes.

In this study, we present *n*-alkane records from surface sediments and sediment core HY04 covering the last 750 ka in the eastern

* Corresponding author. Graduate School of Environmental Studies, Nagoya University, Furo-cho, Chikusa-ku, Nagoya 464-8601, Japan. Fax: +81 52 789 3033.
E-mail address: horikawa@nagoya-u.jp (K. Horikawa).

0033-5894/$ – see front matter
doi:10.1016/j.yqres.2010.01.001

equatorial Pacific (EEP), which is the first high-resolution, continuous record back to the Mid-Pleistocene in the EEP. A key point in this study is that *n*-alkane chain lengths, $C_{31}/(C_{29}+C_{31})$ ratios, exhibit a long-term decrease from MIS 17 to 13 (0.69–0.5 Ma) with outstanding lower values at MIS 13. We have interpreted the long-term decrease in $C_{31}/(C_{29}+C_{31})$ ratios to be a result of decreased input of longer chain length *n*-alkanes transported from northern South America, where hot and dry conditions prevail today, due to the increased humidity in northern South America during MIS 17–13. The anomalously humid period inferred from our records may be associated with unusual environmental conditions during MIS 17 (15)–13 documented in various marine and terrestrial climate archives from around the world (e.g., Guo et al., 2009; Suganuma et al., 2009), implying a regional response to the climate perturbation occurred globally during the Mid-Pleistocene.

Study area

In the EEP, oceanic surface currents are closely related to the intensity and direction of the trade winds, which determine the meridional distribution of sea-surface temperature (SST) and the convective intensity and the latitudinal position of the ITCZ (Fig. 1) (Li and Philander, 1996). These ocean-wind conditions are controlled by changes in seasonal insolation in both hemispheres (Li and Philander, 1996; Srinivasan and Smith, 1996; Timmermann et al., 2007). When the Northern Hemisphere (NH) summer insolation increases, the southeasterly (SE) trade winds intensify and warmer water moves northward. The ITCZ is then displaced northward by ~10°N (Fig. 1). During the periods of the maxima in the Southern Hemisphere (SH) summer insolation, in contrast, the northeasterly (NE) trade winds intensify. At the same time, the meridional SST gradient decreases and the ITCZ moves toward the equator, which is as far south as it extends annually (Fig. 1). Although seasonal insolation change is one of the significant forcings determining ocean-wind conditions and meridional positions of the ITCZ in the EEP and above northern South America, modeling studies suggest that sea and air surface temperature anomalies associated with changes in the Atlantic meridional overturning circulation, continental ice sheets, and sea ice may also be significant determinants on a geological time-scale (e.g., Chiang et al. 2003; Chiang and Bitz, 2005; Broccoli et al. 2006).

Materials and methods

We investigated surface sediments from eight sites along the 95°W transect and sediment core HY04 (core length = 12.3 m; 4°01.66′N, 95°03.45′W; water depth = 3563 m) at the southern edge of the southerly position of the ITCZ, which were taken during the R/V *Hakuho-Maru* cruise KH03-1 (Fig. 1). The lithology of core HY04 is characterized mainly by calcareous ooze with moderate bioturbation and no visible turbidites (Horikawa et al., 2006). The sediments were separated into samples with a thickness of 2.5 cm for each measurement on land. The biogenic components were measured at intervals of 5.0 cm throughout the past 750 ka. We picked 4 to 12 individuals of *Uvigerina* spp. from the >125 μm size fraction and cleaned them ultrasonically in methanol. The isotopic data were generated at CMCR, Kochi University, on a Finnigan MAT 253 isotope ratio mass spectrometer using an automated carbonate device. These data were calibrated with NBS-19. The precision of the measurements was better than 0.06‰ and 0.03‰ (1σ) for $\delta^{18}O$ and $\delta^{13}C$, respectively.

We established an age model for core HY04 based on seven AMS-^{14}C dates and a $\delta^{18}O$ stratigraphy (Fig. 2 and Supplemental data 1). For the $\delta^{18}O$ stratigraphy, we correlated our benthic $\delta^{18}O$ records with the astronomically calibrated *Uvigerina* spp. $\delta^{18}O$ chronology of ODP 677 in the Panama Basin (Shackleton et al., 1990) because both records matched well due to the proximity of core sites. However, around 420 ka, the ODP 677 $\delta^{18}O$ chronology has some discrepancies with the global stacked $\delta^{18}O$ chronology, which has been used recently as a new reference curve (Lisiecki and Raymo, 2005). Therefore, for the lower part of the core (prior to 380 ka) we used the global stacked $\delta^{18}O$ record for the correlation.

For biomarker analysis, the sediment samples were oven dried (60°C) and ground manually for homogenization. We then extracted the lipids in each sample from the dried sediments (1–3 g) with an internal standard (*n*-tetracosane-d_{50} and 18-pentatriacontanone) using an accelerated solvent extractor (ASE-200, Dionex Japan, Ltd.) at 100°C and 1000 psi (extracted twice). A mixture of dichloromethane and methanol (6/4 v/v) was used as the solvent. The lipid extract was separated from the neutral compounds by silica gel column chromatography (SiO_2 with 5% distilled water; id = 5.5 mm; length = 45 mm). Further details on this method are available in Yamamoto et al. (2000). The separated alkenone and alkane fractions were analyzed using an Agilent 6890N gas chromatograph fitted with an on-column injector and a capillary column coated with CP-Sil5CB

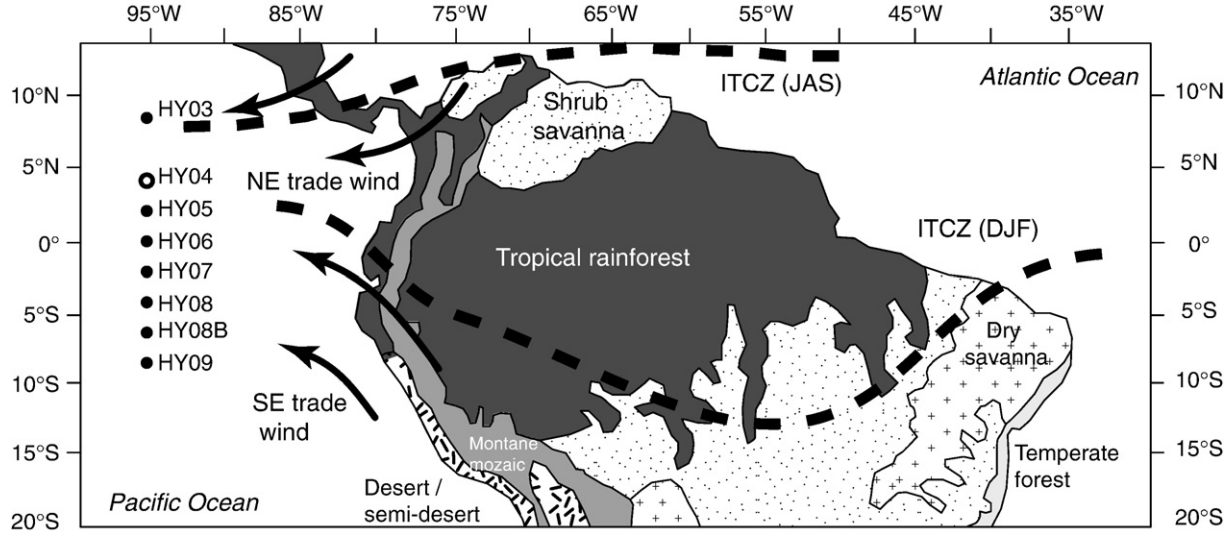

Figure 1. Map of coring sites used in this study. Regional winds and present-day potential vegetation types are also shown. Open circle indicates site HY04 having the long-term trend of *n*-alkane chain lengths discussed in the text. The present-day positions of the Intertropical Convergence Zone (ITCZ) during the northern summer (JAS) and northern winter (DJF) are depicted with a dotted black line. The vegetation map is modified from Jacob et al. (2007).

https://doi.org/10.1016/j.yqres.2010.01.001 Published online by Cambridge University Press

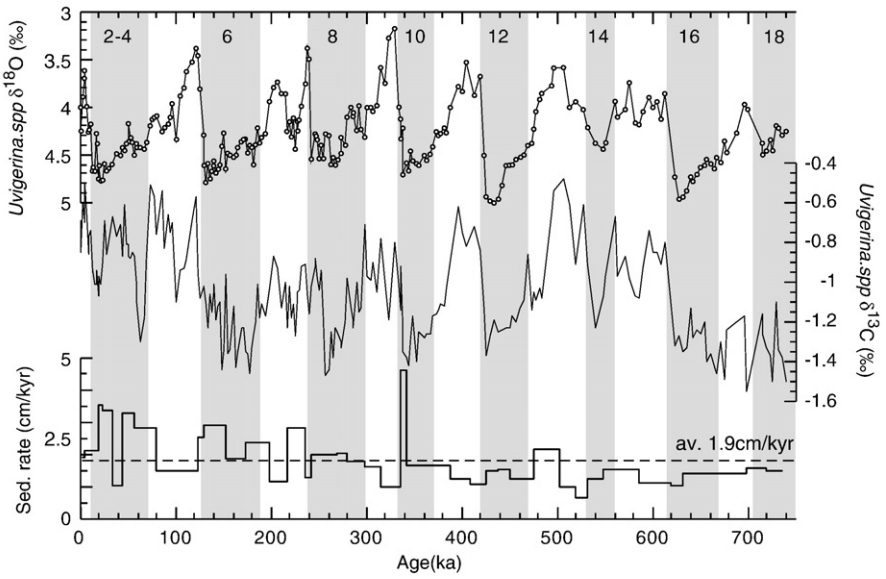

Figure 2. *Uvigerina* spp. $\delta^{18}O$ and $\delta^{13}C$ records from core HY04. Vertical shaded bars indicate glacial intervals. Marine oxygen isotope stages (MIS) are noted along the *x*-axis. The bottom panel shows sedimentation rates. The $\delta^{18}O$ and $\delta^{13}C$ data are given in the auxiliary material for this article.

(60 m; id = 0.25 mm; thickness = 0.25 μm). Helium was used as a carrier gas. For the alkane fraction, oven temperature was programmed to increase from 70° to 130°C at 20°C/min, from 130° to 310°C at 4°C/min, and then remain constant at 310°C for 15 min. The oven program for the alkenone fraction followed Horikawa et al. (2006). Both fractions were quantified by gas chromatography with flame-ionization detection relative to the concentration of the internal standard. Triplicate analyses (from extraction to measurements) of a standard EEP sediment indicated standard deviations (1σ) of ±14% for alkenone content, ±15% for alkane content, and ±0.02

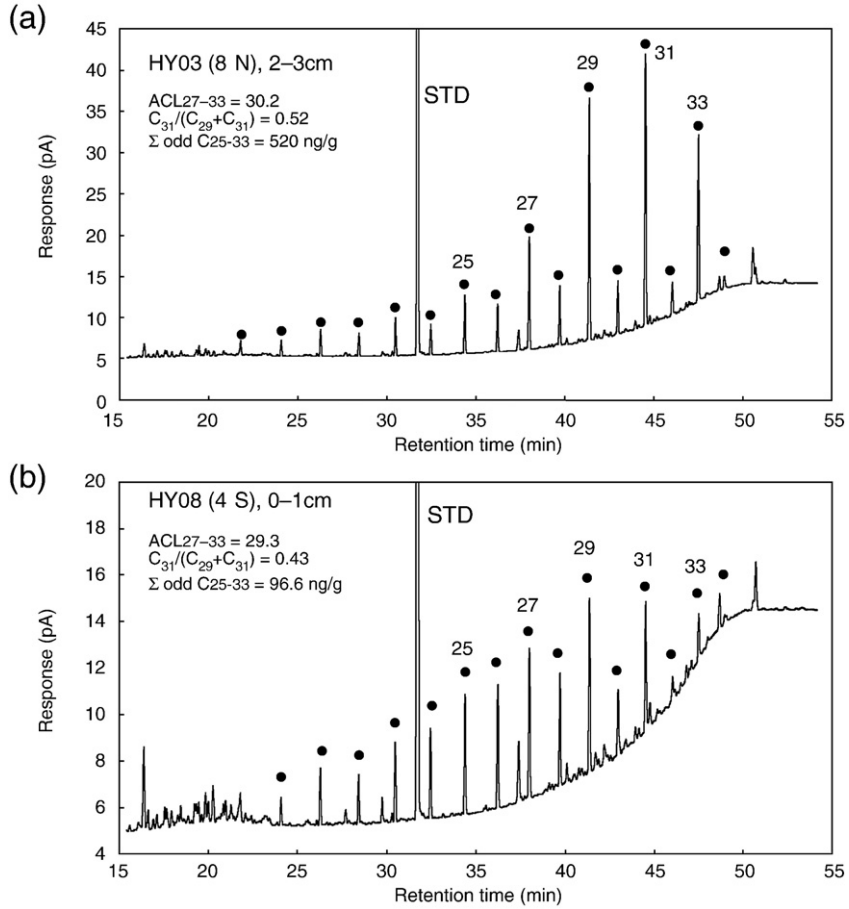

Figure 3. Gas chromatographic traces of saturated hydrocarbon fractions of organic solvent extracts of surface sediment samples with (a) a high chain length (site HY03) and (b) a low chain length (site HY08). The carbon number maximum of the *n*-alkanes moves from C_{31} at the northern sites to C_{29} further south. Dots indicate *n*-alkanes and odd *n*-alkane C_{25-33} are noted.

https://doi.org/10.1016/j.yqres.2010.01.001 Published online by Cambridge University Press

(2σ) for the *n*-alkane $C_{31}/(C_{29}+C_{31})$ ratio. This analytical error was minor compared to the meridional changes and downcore changes in *n*-alkane $C_{31}/(C_{29}+C_{31})$ ratios discussed in this study.

Results

n-Alkanes

The *n*-alkanes extracted from surface sediments along the 95°W transect and core HY04 ranged in carbon number from *n*-C_{19} to *n*-C_{34} with a predominance of odd over even carbon-numbered-homologues (Fig. 3). The distributions of *n*-alkanes were unimodal, and *n*-C_{29} or *n*-C_{31} alkanes were the most abundant (Fig. 3).

For the surface sediments, the sum of odd *n*-C_{25-33} alkane concentrations ($\sum$odd *n*-C_{25-33} alkanes) are 58 to 728 ng/g, showing a meridional change with the highest value at site HY03 (8°N) below the annual mean position of the ITCZ and the lowest value at site HY09 (8°S) (Table 1 and Fig. 4). The $\sum$odd *n*-C_{25-33} alkane records are consistent with meridional distributions of land-derived ^{232}Th fluxes along the 110°W and 140°W transects reported by Anderson et al. (2006) and McGee et al. (2007), although our data are not fluxes. Furthermore, the *n*-alkane $C_{31}/(C_{29}+C_{31})$ ratios decrease from site HY03 (0.52) to site HY05–HY09 (0.38–0.47, av. 0.43); the carbon number maximum of the *n*-alkanes change from C_{31} at the northern sites to C_{29} further south (Figs. 3 and 4). The average chain length (ACL) parameter (Poynter et al., 1989) also decreases southward in parallel with the $C_{31}/(C_{29}+C_{31})$ ratios (Fig. 4). In addition, odd versus even carbon-number predominance (carbon preference index (CPI)) values ranging from 1.5 to 4.6 also show a north–south trend, with lower CPI values at the southern sites (HY05–HY09). These *n*-alkane abundances and carbon number distributions change significantly across the southern edge of the ITCZ between sites HY04 (4°N) and HY05 (2°N).

For core HY04, the $\sum$odd *n*-C_{25-33} alkanes range from 34 to 289 ng/g over the past 750 ka, and on the whole, the $\sum$odd *n*-C_{25-33} alkanes decrease with depth (Fig. 5 and Supplemental data 2). The CPI index is 2.2 to 5.8 (av. 4.1). Furthermore, *n*-alkane $C_{31}/(C_{29}+C_{31})$ ratios vary from 0.42 to 0.6 (av. 0.53), which correlate with downcore changes in the ACL ($r^2=0.69$ ($p<0.001$)). Both chain length parameters appear to show systematic glacial–interglacial (G–IG) variations with lower interglacial and higher glacial values (Fig. 5). More importantly, in addition to the G–IG oscillations, there is a long-term decrease in the $C_{31}/(C_{29}+C_{31})$ ratios during MIS 17–13 (0.69–0.5 Ma) with outstanding lower values at MIS 13.

Alkenone-derived SST

Alkenones are uniquely synthesized by several species of haptophyte algae (Genera *Gephyrocapsa* and *Emiliania*) (Marlowe et al., 1990; Herbert, 2003). We were unable to precisely quantify alkenone content and alkenone-derived SST from surface sediments due to low abundance of alkenones in the sediments, as reported by Prahl et al. (2006). Alkenone-SST of the uppermost Holocene sample was within the annual mean SSTs in the surface (0–10 m), and thus we equated alkenone-derived SST from core HY04 with mean annual SST (Horikawa et al., 2006). Downcore SST changes show less variability over the past ~240 ka (MIS 7) and greater relative amplitude in SSTs (up to ~2°C) from MIS 8 to MIS 13, and again less G–IG amplitude from MIS 14 to MIS 18. The maximum SST (27.2°C) occurs at 126 ka during MIS 5e, and the minimum SST (24.3°C) occurs at 442 ka during MIS 12 (Fig. 5). Our alkenone-derived SSTs have a first-order trend similar to that of the alkenone-derived SST records from the cold-tongue in the EEP (ODP 846B, 3°5′S, 90°49′W) (Liu and Herbert, 2004).

The sum of $C_{37:2}$ and $C_{37:3}$ (di- and tri-unsaturated ketones) concentrations ($\sum C_{37}$) are 0.01 to 5.8 μg/g-sediment (av. 1.6 μg/g-

Table 1
n-Alkane data from surface sediments along the 95°W transect. *n*-C_{34} was below detection limit. $CPI_{27-33}=0.5[(C_{27}+C_{29}+C_{31}+C_{33})/(C_{26}+C_{28}+C_{30}+C_{32})+(C_{27}+C_{29}+C_{31}+C_{33})/(C_{28}+C_{30}+C_{32}+C_{34})]$. $ACL_{27-33}=[27(C_{27})+29(C_{29})+31(C_{31})+33(C_{33})]/(C_{27}+C_{29}+C_{31}+C_{33})$.

Site	Depth (cm)	*n*-C_{23} (ng/g-sed)	*n*-C_{24} (ng/g-sed)	*n*-C_{25} (ng/g-sed)	*n*-C_{26} (ng/g-sed)	*n*-C_{27} (ng/g-sed)	*n*-C_{28} (ng/g-sed)	*n*-C_{29} (ng/g-sed)	*n*-C_{30} (ng/g-sed)	*n*-C_{31} (ng/g-sed)	*n*-C_{32} (ng/g-sed)	*n*-C_{33} (ng/g-sed)	Odd C_{25-33} (ng/g-sed)	$C_{31}/(C_{29}+C_{31})$ raw	$C_{31}/(C_{29}+C_{31})$ corr	ACL_{27-33}	CPI_{27-33}
HY03MC	0–2	43.73	36.25	62.72	49.06	102.43	52.08	207.88	45.17	221.55	25.46	133.22	727.8	0.52	–	30.2	4.6
HY04MC	0–2	11.63	13.53	20.86	18.84	30.47	18.21	52.60	13.91	54.75	7.59	32.75	191.4	0.51	–	30.1	3.6
HY05MC	0–1	8.31	10.21	15.98	16.93	19.84	14.90	21.24	8.69	15.47	3.04	6.97	79.5	0.42	0.40	29.3	1.9
HY06MC	0–1	11.48	16.09	25.41	28.33	29.83	22.78	25.04	12.52	15.15	3.58	5.46	100.9	0.38	(-0.15)	28.9	1.5
HY07MC	0–1	9.79	8.89	13.78	13.40	16.62	11.47	20.87	7.09	18.55	2.83	5.93	75.7	0.47	0.50	29.4	2.3
HY08MC	0–1	11.68	12.83	18.27	19.28	23.50	17.48	27.09	10.89	20.28	3.44	7.45	96.6	0.43	0.42	29.3	2.0
HY08BMC	0–1	10.47	13.31	19.10	19.59	22.79	17.25	26.74	11.83	21.32	4.19	6.78	96.7	0.44	0.46	29.3	1.9
HY09MC	0–2	5.68	7.66	11.70	11.57	14.37	9.17	16.42	4.86	11.91	1.44	3.28	57.7	0.42	0.41	29.2	2.3

https://doi.org/10.1016/j.yqres.2010.01.001 Published online by Cambridge University Press

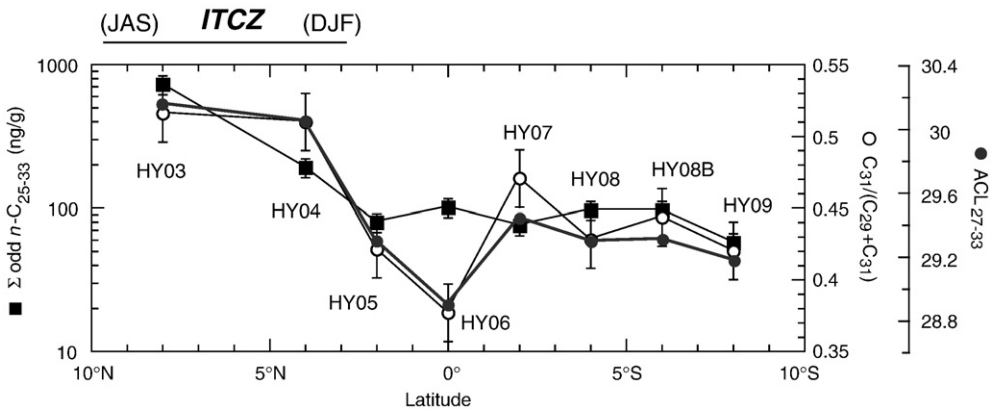

Figure 4. Meridional changes in odd *n*-alkane C_{25-33} concentration (with 1σ error) and *n*-alkane chain length ($C_{31}/(C_{29}+C_{31})$) and ACL_{27-33} (with 2σ error) of surface sediments along the 95°W transect (see Fig. 1). Variability of *n*-alkane $C_{31}/(C_{29}+C_{31})$ ratios across the southern edge of the ITCZ exceeds the analytical error. Site HY03 (at 8°N) is characterized by the highest abundance of the odd *n*-alkane C_{25-33} because of intense precipitation scavenging of dust within the ITCZ.

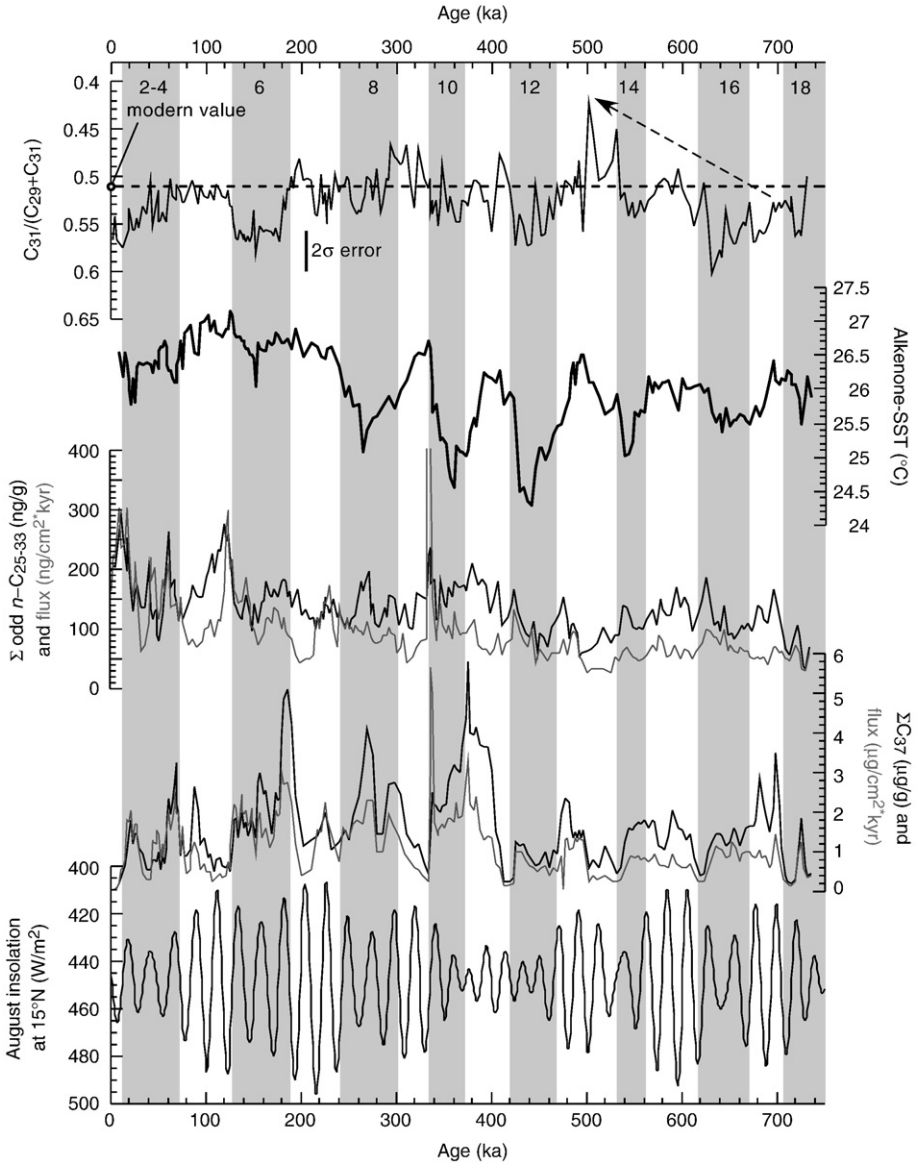

Figure 5. The *n*-alkane $C_{31}/(C_{29}+C_{31})$ ratios (note *y*-axis is inverted), alkenone-derived SST, $\sum$odd *n*-alkane C_{25-33} concentration and flux, alkenone (C_{37}) concentration and flux records from core HY04 over the last 750 ka. Some minimum periods of the Northern Hemisphere (NH) summer insolation (august, 15°N) (Berger and Loutre, 1991) correspond to higher alkenone abundance. Note that the *n*-alkane $C_{31}/(C_{29}+C_{31})$ ratios clearly show a long-term decrease during MIS 17–13 (0.69–0.5 Ma) with outstanding lower values at MIS 13.

https://doi.org/10.1016/j.yqres.2010.01.001 Published online by Cambridge University Press

sediment) over the past 750 ka (Fig. 5). Unlike the ∑odd n-C_{25-33} alkanes, the ∑C_{37} records clearly show precession-related variability, especially until the past 300 ka (Fig. 5).

Discussion

Meridional variation in n-alkane abundances and n-alkane chain lengths

From the higher abundance of odd-numbered homologues relative to their even-numbered counterparts and maximum abundance in n-C_{29} or n-C_{31}, long-chain n-alkanes are considered to be primarily derived from land plant epicuticular waxes (e.g., Eglinton and Hamilton, 1967). Given the location of cores within the sphere of influence of the trade winds and the absence of major rivers near core sites, odd n-C_{25-33} alkanes in our sediments can be interpreted to be supplied by eolian transport.

In the equatorial Pacific, dust is efficiently scavenged by precipitation within the ITCZ (Zender et al., 2003). Scavenging of dust within the ITCZ explicitly prohibits the long-distance transport of dust, as shown by the significant decrease of land-derived ^{232}Th fluxes from ~0.7 μg/cm^2 kyr at 110°W to 0.3 μg/cm^2 kyr at 140°W (Anderson et al., 2006; McGee et al., 2007). Yet, their data also show meridional variations quite similar to our n-alkane abundances at the 95°W transect. These common N–S trends of dust, which are observed from the eastern to the central equatorial Pacific, may be explained mainly by efficient scavenging of dust within the ITCZ and dust production, which depends on vegetation density, in both hemispheres.

Since long-chain n-alkanes are primarily derived from land plant epicuticular waxes, we can suppose that the meridional variations in n-alkane chain lengths also provide information on land plant-derived n-alkanes. Yet, we should consider that low CPI values (1.5–2.3) are observed at southern sites (HY05–HY09). Since low CPI values of n-alkanes are often regarded as the influence of contamination such as vehicle exhaust (Simoneit, 1984), fuel or wood burning (Standley and Simoneit, 1987), or even marine sources (Lichtfouse et al., 1994), there arises a possibility that the primary carbon number distributions of land plant-derived n-alkanes are modified. Given that the southern sites are characterized by extremely low abundances in the ∑odd n-C_{25-33} alkanes compared to those of northern sites, contamination might exert greater influence on the southern sites than on the northern sites, and create the observed meridional changes in n-alkane chain lengths.

Hayakawa et al. (1996) and Ternois et al. (1998) have reported that marine sinking particles (i.e., algae and bacteria) at Freid Bay and Southern Ocean, respectively, contain n-alkanes distributed from n-C_{20} to n-C_{35} with low CPI values from 1.0 to 1.9. Given that lower CPI values (1.5–2.3) are observed at the southern sites (HY05–HY09) where marine productivity is relatively high in the EEP, additional input from such marine sources may modify primary carbon number distributions of land plant-derived n-alkanes. Yet, marine sources are characterized by mid n-alkane (n-C_{15-22}) predominance, and n-C_{29} or n-C_{31} alkanes are minor components, suggesting that overprinting of marine sources is not a significant factor altering the relative abundances of n-C_{29} and n-C_{31}. Fossil fuels also have a low CPI value (~1) and are considered to be another potential contaminant phase for southern sites. Since fossil fuels are characterized by a unimodal distribution with n-C_{26} or n-C_{28} predominance (Lichtfouse and Eglinton, 1995), contamination might affect primary n-alkane $C_{31}/(C_{29}+C_{31})$ ratios. Accordingly, their potential influence should be evaluated before using $C_{31}/(C_{29}+C_{31})$ ratios. Here, we assume that fossil fuels have a unimodal distribution with n-C_{28} predominance, and estimated average contaminant ratios of n-C_{29} and n-C_{31} relative to n-C_{28} based on the linearly decrease trend from n-C_{28} to n-C_{32} using the data from HY03 and HY04. Using these rates, we calculated corrected $C_{31}/(C_{29}+C_{31})$ ratios for southern sites. As a consequence, except for HY06 (CPI = 1.5), sites HY05–HY09 (CPI = 1.9–2.3) did not show significant differences between raw $C_{31}/(C_{29}+C_{31})$ and corrected $C_{31}/(C_{29}+C_{31})$ ratios (Table 1), which means that meridional changes in n-alkane $C_{31}/(C_{29}+C_{31})$ ratios are not an artifact of the influences of fossil fuels on southern sites. Downcore changes in CPI (2.2–5.8, av. 4.1) exceed this criterion (CPI > 1.9), and thus they are not interpreted as artifacts of fossil fuel contamination.

Gregory et al. (1999) found that northern-source pollutants exhibit very steep gradients across the ITCZ, and they discussed how interhemispheric dust transport is highly limited because of precipitation scavenging in the ITCZ. Existing Nd and Pb isotopes (Jones et al., 1994; Jones et al., 2000) and clay mineralogy data (Griffin et al., 1968; Prospero and Bonatti, 1969), as well as dust models (Luo et al., 2003), suggest a change from northern-source to southern-source dust between 5°N and 0°N in the equatorial Pacific. Given these studies, it is reasonable to conclude that the differences in n-alkane $C_{31}/(C_{29}+C_{31})$ ratios across the southern edge of the ITCZ reflect primarily different northern and southern signals concerning carbon number distributions of land plant-derived n-alkanes.

n-Alkane chain length index

Long-chain, odd-numbered n-alkanes are produced as moisture-regulating epicuticular leaf waxes (Tulloch, 1976). Dodd et al. (1998), Dodd and Rafii (2000), and Shepherd and Griffiths (2006) reveal that plants tend to synthesize longer chain length alkanes under water stress conditions to provide a more efficient wax coating. Indeed, n-alkane chain length indices (n-alkane $C_{31}/(C_{29}+C_{31})$ ratio and ACL) of C_4-type plants, which are common in hot and dry environments, exhibit distribution maxima in n-C_{31} or n-C_{33}, whereas C_3-type plants exhibit distribution maxima in n-C_{29} or n-C_{31} (Boom et al., 2002; Rommerskirchen et al., 2006; Vogts et al., 2009). These findings suggest that n-alkane chain lengths are related to vegetation changes and, thus, to ambient temperature and/or aridity (Dodd and Rafii, 2000; Rommerskirchen et al., 2003).

Taking these studies on n-alkane chain lengths into account, we can interpret that longer n-alkane chain lengths observed at HY03 and HY04, which are influenced mainly by NE trade winds, reflect a contribution of higher land plants growing under high ambient temperature and/or aridity. Indeed, an integrated vegetation map represents that C_4-type plants of savannas are abundant in northern South America (Still et al., 2003) (Fig. 1), which is the upwind region of the NE trade winds. For this reason, it is possible that C_4-type plants and C_3-type plants (e.g., C_3 species of savannas) adapted to hot and dry environments in northern South America are responsible for longer chain lengths of n-alkanes at the northern sites. In contrast, given that the southern sites are influenced by SE trade winds, the shorter chain lengths of the n-alkanes at the southern sites (HY05–HY09) are interpreted to reflect a contribution of higher land plants growing under more temperate conditions. A potential source may be tropical-subtropical high-altitude C_3-type grassland (paramo) in western South America (Clapperton, 1993; Mora and Pratt, 2002; Still et al., 2003).

n-Alkane chain lengths on G–IG cycles

Downcore n-alkane $C_{31}/(C_{29}+C_{31})$ ratios exhibit low correlation with the CPI index ($r^2 = 0.34$ ($p < 0.001$)). This implies that potential overprinting of marine algae, bacteria, and fossil fuels is a minor factor in downcore variability of n-alkane $C_{31}/(C_{29}+C_{31})$ ratios.

Previous studies in the Cariaco Basin off Venezuela (10°N) reveal that C_4 plants expanded during the LGM and stadials (e.g., Hughen et al., 2004; González et al., 2008). At 5°N in Andean Colombia, δ^{13}C values of paleosol organic matter exhibit elevated δ^{13}C values indicative of C_4 plants during the LGM (Mora and Pratt, 2002), suggesting that C_4 plants expanded into the high-altitude C_3 grassland. Ice cores and lacustrine sediments in South America reveal

https://doi.org/10.1016/j.yqres.2010.01.001 Published online by Cambridge University Press

that northern Brazil (3°S) and Huascaran in Peru (9°S) were drier during the LGM (Thompson et al., 2000; Jacob et al., 2007) and the Altiplano of Bolivia (17°S) and Sajama in Bolivia (18°S) were wetter during the LGM (Baker et al., 2001; Thompson et al., 2000). These vegetation and arid/humid changes in northern South America during the LGM are interpreted to be related to southerly latitudinal displacements of the precipitation zone associated with the ITCZ (e.g., Wang et al., 2004, 2007; Cruz et al., 2005). Clearly, a land region ranging from 10°N to 9°S, which is the potential source region of higher plant waxes for our study site, was drier during the LGM, driving expansion of C_4 plants. Model studies show that during glacial periods expansion of the ice sheet and sea-ice in the northern high latitudes produced a significant latitudinal temperature contrast and intensified the NE trade wind field during boreal winter (Chiang et al., 2003; Chiang and Bitz, 2005; Broccoli et al., 2006). Given these conditions, land plant-derived *n*-alkanes in core HY04 during glacial periods are considered to be of northern South American origin. Therefore, the longer chain lengths observed in core HY04 in glacial periods might show that northern South America experienced expansion of drier environments during glacial periods (at least the LGM), which corroborates the conclusion of previous studies.

In the case of northern South America, previous studies strongly suggest that drier conditions due to the southerly displaced ITCZ may have been the primary trigger of proliferation of C_4 plants (Hughen et al., 2004; Wang et al., 2004). Regional climate may have exerted even greater control than pCO_2 (a 30% decrease during the LGM, Street-Perrott et al., 1997; Huang et al., 1999) over the relative abundance of C_3 and C_4 plants during the LGM (Huang et al., 2001; Zhang et al., 2003).

Long-term decrease in n-alkane $C_{31}/(C_{29}+C_{31})$ ratios during MIS 17–MIS 13

In addition to the G–IG oscillations in *n*-alkane $C_{31}/(C_{29}+C_{31})$ ratios, there is a marked long-term decrease from MIS 17 to 13 (Fig. 6). Like the cause of the G–IG oscillations in *n*-alkane $C_{31}/(C_{29}+C_{31})$ ratios, chain lengths of core HY04 might be related to anomalous changes in temperature or aridity/humidity in adjacent land. Further, given that site HY04 lies at the southern edge of the southerly position of the ITCZ, changes in northern- and southern-sources of dust in response to changes in meridional position of the ITCZ are also interpreted to be a potential cause of the long-term decrease in *n*-alkane $C_{31}/(C_{29}+C_{31})$ ratios.

Some marine archives from the western equatorial Pacific (Medina-Elizalde and Lea, 2005) and the southern Atlantic (Becquey and Gersonde, 2003) show cooler SSTs at MIS 13 than for other interglacials of the Mid-Pleistocene. This anomalous cooler condition might have resulted in decreases in chain lengths. Yet, SST evolution around MIS 13 is not uniform in the equatorial regions. SST records from the South China Sea (SCS) show relatively constant interglacial SST evolution during MIS 17–13 (Shyu et al., 2001; Li et al., 2008). Moreover, in the heart of the cold tongue of the EEP, SSTs are almost constant for interglacial periods during MIS 17–13, although glacial SSTs gradually decreased (Liu and Herbert, 2004), which is confirmed by our SST record from the northern edge of the EEP cold tongue (Fig. 5). Unfortunately, there are no long-term SST records from the western equatorial Atlantic (WEA) adjacent to northern South America. Yet, given that the equatorial regions did not experience long-term interglacial cooling from MIS 17 to MIS 13, we speculate that northern South America was not subject to long-term cooling during the period. Thus, the possibility that the long-term decrease in *n*-alkane $C_{31}/(C_{29}+C_{31})$ ratios during MIS 17–13 was related to cooling on land seems unlikely. Rather, as discussed below, we propose that reorganized atmospheric circulations during and shortly after the MPT may have affected moisture transport from ocean to land.

It is well known that magnetic and grain-size parameters in paleo-soil/loess sequences in China during MIS 15–MIS 13 show formation of well-developed soils indicative of a warm-humid

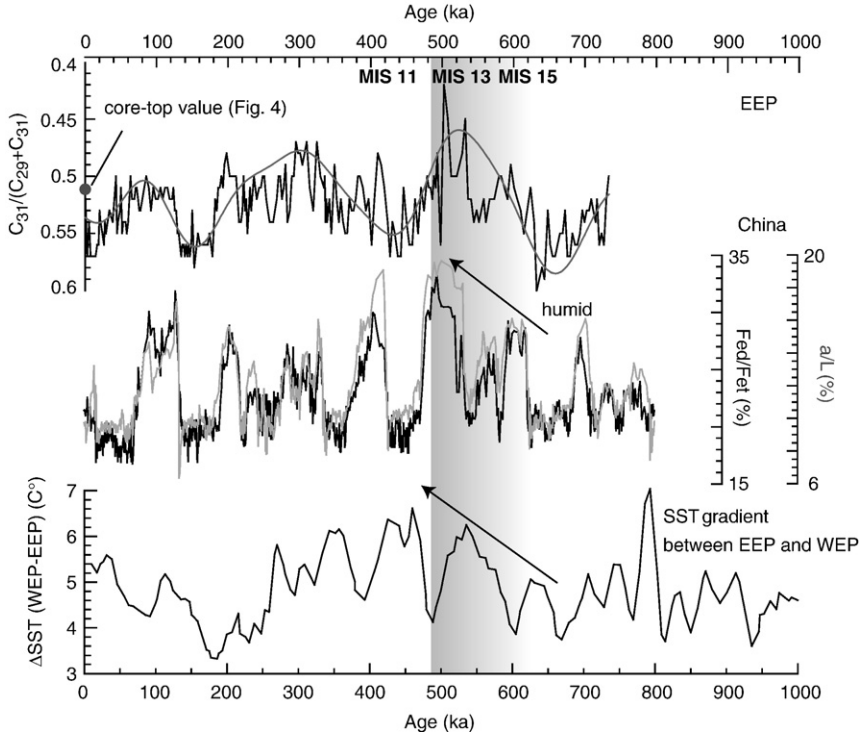

Figure 6. Comparison of the $C_{31}/(C_{29}+C_{31})$ record from core HY04 with Fed/Fet (%) and a/L (%) (Guo et al., 2009), and the ΔSST between MD97-2140 from the western Equatorial Pacific and ODP 846 from the cold-tongue in the EEP (de Garidel-Thoron et al., 2005; Liu and Herbert, 2004). Chemical weathering indices Fed/Fet (%) and a/L (%) in the Loess Plateau primarily depend on the monsoon-related summer moisture and temperature, which are used as proxies of Asian summer monsoon activity (see details in Guo et al., 2009). The long-term trend in *n*-alkane chain lengths was obtained by Gaussian-filtering (central frequency: 0.004 cycles/kyr, bandwidth: 0.004 cycles/kyr).

https://doi.org/10.1016/j.yqres.2010.01.001 Published online by Cambridge University Press

climate. Recently published chemical weathering indices of China loess, which are widely used to document effects of the summer monsoon because soil formation and chemical weathering in the Loess Plateau depend primarily on monsoon-related summer moisture and temperature, exhibit the strongest peak at MIS 13 (Guo et al., 2000, 2009) (Fig. 6). These records and other previous studies strongly suggest that intensification of Asian summer monsoon activity and related warm-humid climate conditions in the Asia monsoon regions occurred throughout MIS 15–MIS 13 (e.g., Kukla and Cilek, 1996; Sun et al., 2006; Suganuma et al., 2009). Yet, the principal cause of the intense monsoon activity has not been considered to be a result of astronomical forcing because summer insolation weakened at MIS 13 (Fig. 5). Interestingly, the zonal surface thermal gradient between the western and eastern equatorial Pacific increased from MIS 17 to MIS 13 (de Garidel-Thoron et al., 2005) (Fig. 6). It is possible that the increased zonal SST gradient was driven by an intensification of Walker circulation. The intensified Walker circulation may have enhanced moisture advection from the ocean to land during this period (i.e., western equatorial Pacific warm pool to Asia and the equatorial Atlantic warm pool to northern South America). Indeed, Shyu et al. (2001) documented that the SCS experienced extremely lower sea-surface salinity conditions during MIS 13, and data from the Ceara Rise in the equatorial Atlantic show unusually high precipitation in the Amazon Basin during MIS 13 (Harris et al., 1997). Both records imply intensified onshore moisture transport at the time. These available records let us to propose the most likely scenario that the intensified Walker circulation caused moisture advection from the equatorial Atlantic warm pool to northern South America to enhance, and then arid regions in northern South America shifted to humid regions. This hypothesis seems to explain the long-term decrease in *n*-alkane $C_{31}/(C_{29}+C_{31})$ ratios from MIS 17 to MIS 13 with the outstanding lower values at MIS 13.

Alternatively, we have to carefully consider latitudinal positions of the ITCZ. In the EEP, the alkenone-derived SST records from the cold-tongue clearly show a long-term, glacial SST cooling during the Mid-Pleistocene (Liu and Herbert, 2004) (Fig. 5), indicating that the SE trade winds intensified gradually. In the eastern equatorial Atlantic, strong SE trade winds strengthened return flow of warm surface waters from the western into the eastern tropical Atlantic and resulted in long-term SST increases in Angola Basin during 0.9–0.55 Ma (Schefuß et al., 2004). If the SE trade winds intensified gradually during and just after the MPT, as shown by SST proxies, latitudinal positions of the ITCZ might have gradually shifted northward at the time and site HY04 was located south of the ITCZ under the influence of the SE trade winds. If so, the long-term decrease in *n*-alkane $C_{31}/(C_{29}+C_{31})$ ratios during MIS 17–MIS 13 can be explained by the gradual increase in southern-source *n*-alkanes with shorter chain lengths. This alternative scenario seems to be corroborated by the lower abundance of $\sum$odd *n*-C_{25-33} alkanes during the period. Yet, it should be noted that our alkenone-derived SST and abundance records exhibit relatively warm conditions and low abundance during MIS 13, which seem to conflict with the expectation of the intensified SE trade winds and attendant enhanced upwelling at MIS 13 (Fig. 5). Therefore, we interpret that northward displacement of the ITCZ in the EEP may not have occurred during MIS 13, although the SE trade winds might have been intensified gradually at glacials.

A comparison with various marine and terrestrial climate archives from around the world corroborates that unusual environmental conditions prevailed throughout MIS 17(15)–MIS 13. In particular, low- to mid-latitude regions under the influence of Asian and African monsoons experienced significant changes in precipitation zone and in precipitation intensity (e.g., Guo et al., 2009). These changes may have been related to changes in the atmospheric circulation regime (i.e., Walker circulation and trade winds).

Conclusions

Plants tend to synthesize longer chain length *n*-alkanes under water stress conditions in response to increased temperature and/or aridity. From the close relationship between chain lengths and temperature/aridity, we interpreted longer glacial *n*-alkane chain lengths to be a result of expansion of arid conditions in northern South America, which is corroborated by previous studies. Furthermore, the long-term decrease of the *n*-alkane $C_{31}/(C_{29}+C_{31})$ ratios was observed from MIS 17 to MIS 13 (0.69–0.5 Ma). During the Mid-Pleistocene, increased zonal SST gradient in the equatorial Pacific suggests that intensified Walker circulation may have enhanced moisture advection from the equatorial Atlantic warm pool to adjacent northern South America. This process may have reduced arid regions and increased humid regions in northern South America, which may have increased the relative contribution of shorter chain lengths of *n*-alkanes, adapted to humid conditions, transported from northern South America during MIS 17–13. This finding indicates that changes in atmospheric circulations during and shortly after the MPT caused drastic vegetation changes. Further, this study highlights that *n*-alkane chain length proxy is useful to shed light on potential regions and specific times in which land climate and attendant vegetation changes occurred. Yet, to quantitatively discuss relative abundances of C_3 and C_4 plants, molecular δD and $\delta^{13}C$ of the *n*-alkanes are required.

Acknowledgments

We thank Y. Takeda and S. Yanagimoto for handpicking of foraminifera and the scientists who participated in the R/V *Hakuho-Maru* cruise KH03-1 for their help during coring. This work was supported by a JSPS research fellowship for young scientists to K.H. (No. 15050041), the Sasakawa Scientific Research Grant from The Japan Science Society, and 21st-Century Center of Excellence Program (E-01, Graduate School of Environmental Earth Science, Hokkaido University) of MEXT. This paper received the substantial benefit of many constructive comments from anonymous reviewers and the editor.

Appendix A. Supplementary data

Supplementary data associated with this article can be found, in the online version, at 10.1016/j.yqres.2010.01.001.

References

Anderson, R.F., Fleisher, M.O., Lao, Y., 2006. Glacial–interglacial variability in the delivery of dust to the central equatorial Pacific Ocean. Earth and Planetary Science Letters 242, 406–414.

Baker, P.A., Rigsby, C.A., Seltzer, G.O., Fritz, S.C., Lowenstein, T.K., Bacher, N.P., Veliz, C., 2001. Tropical climate changes at millennial and orbital timescales on the Bolivian Altiplano. Nature 409, 698–701.

Becquey, S., Gersonde, R., 2003. A 0.55-Ma paleotemperature record from the Subantarctic zone: implications for Antarctic Circumpolar Current development. Paleoceanography 18, 1014. doi:10.1029/2000PA000576.

Berger, A., Loutre, M.F., 1991. Insolation values for the climate of the last 10 million years. Quaternary Science Reviews 10, 297–317.

Boom, A., Marchant, R., Hooghiemstra, H., Sinninghe Damsté, J.S., 2002. CO_2- and temperature-controlled altitudinal shifts of C_4- and C_3-dominated grasslands allow reconstruction of palaeoatmospheric pCO_2. Palaeogeography, Palaeoclimatology, Palaeoecology 177, 151–168.

Broccoli, A.J., Dahl, K.A., Stouffer, R.J., 2006. Response of the ITCZ to Northern Hemisphere cooling. Geophysical Research Letters 33, L01702. doi:10.1029/2005GL024546.

Chiang, J.C., Biasutti, M., Battisti, D.S., 2003. Sensitivity of the Atlantic intertropical convergence zone to last glacial maximum boundary conditions. Paleoceanography 18, 1094. doi:10.1029/2003PA000916.

Chiang, J.C., Bitz, C.M., 2005. Influence of high latitude ice cover on the marine Intertropical Convergence Zone. Climate Dynamics 25, 477–496. doi:10.1007/s00382-005-0040-5.

Clapperton, C.M., 1993. Nature of environmental changes in South America at the Last Glacial Maximum. Palaeogeography, Palaeoclimatology, Palaeoecology 101, 189–208.

Conte, M.H., Weber, C.J., 2002. Plant biomarkers in aerosols record isotopic discrimination of terrestrial photosynthesis. Nature 417, 639–641.
Cruz, F.W., Burns, S.J., Karmann, I., Sharp, W.D., Vuille, M., Cardoso, A.O., Ferrari, J.A., Dias, P.L.S., Viana, O., 2005. Insolation driven changes in atmospheric circulation over the past 116,000 years in subtropical Brazil. Nature 434, 63–66.
de Garidel-Thoron, T., Rosenthal, Y., Bassinot, F., Beaufort, L., 2005. Stable sea surface temperatures in the western Pacific warm pool over the past 1.75 million years. Nature 433, 294–298.
Dodd, R.S., Rafii, Z.A., 2000. Habitat-related adaptive properties of plant cuticular lipids. Evolution 54, 1438–1444.
Dodd, R.S., Rafii, Z.A., Power, A.B., 1998. Ecotypic adaptation in Austrocedrus chilensis in cuticular hydrocarbon composition. New Phytology 138, 699–708.
Dupont, L.M., Donner, B., Schneider, R., Wefer, G., 2001. Mid-Pleistocene environmental change in tropical Africa began as early as 1.05 Ma. Geology 29, 195–198.
Eglinton, J.R., Hamilton, R.J., 1967. Leaf epicuticular waxes. Science 156, 1322–1335.
Gagosian, R.B., Peltzer, E.T., Merrill, J.T., 1987. Long-range transport of terrestrially derived lipids in aerosols from the South Pacific. Nature 325, 800–803.
González, C., Dupon, L.M., Behling, H., Wefer, G., 2008. Neotropical vegetation response to rapid climate changes during the last glacial period: palynological evidence from the Cariaco Basin. Quaternary Research 69, 217–230.
Gregory, G.L., Westberg, D.J., Shipham, M.C., Blake, D.R., Newell, R.E., Fuelberg, H., Talbot, E.R.W., Heikes, B.G., Atlas, E.L., Sachse, G.W., Anderson, B.A., Thornton, D.C., 1999. Chemical characteristics of Pacific tropospheric air in the region of the Intertropical Convergence Zone and South Pacific Convergence Zone. Journal of Geophysical Research 104 (D5), 5677–5696.
Griffin, J.J., Windom, H., Goldberg, E.D., 1968. The distribution of clay minerals in the world ocean. Deep-Sea Research 15, 433–459.
Guo, Z.T., Biscaye, P., Wei, L.Y., Chen, X.F., Peng, S.Z., Liu, T.S., 2000. Summer monsoon variations over the last 1.2 Ma from the weathering of loess-soil sequences in China. Geophysical Research Letters 27, 1751–1754.
Guo, Z.T., Berger, A., Yin, Q.Z., Qin, L., 2009. Strong asymmetry of hemispheric climates during MIS-13 inferred from correlating China loess and Antarctic ice records. Climate of Past 5, 21–31.
Harris, S.E., Mix, A.C., King, T., 1997. Biogenic and terrigenous sedimentation at Ceara Rise, western tropical Atlantic, supports Pliocene–Pleistocene deep-water linkage between hemispheres. Proceedings ODP, Scientific Results 154, 331–345.
Hayakawa, K., Handa, N., Ikuta, N., Fukuchi, M., 1996. Downward fluxes of fatty acids and hydrocarbons during a phytoplankton bloom in the austral summer in Breid Bay, Antarctica. Organic Geochemistry 24, 511–521.
Herbert, T.D., 2003. Alkenone paleotemperature determinations. In: Elderfield, H. (Ed.), The Oceans and Marine Geochemistry, Treatise on Geochemistry, 6. Elsevier-Pergamon, Oxford, pp. 391–432.
Horikawa, K., Minagawa, M., Murayama, M., Kato, Y., Asahi, H., 2006. Spatial and temporal sea-surface temperatures in the eastern equatorial Pacific over the past 150 kyr. Geophysical Research Letters 33, 13605. doi:10.1029/2006GL025948.
Huang, Y., Street-Perrott, F.A., Perrott, F.A., Metzger, P., Eglinton, G., 1999. Glacial–interglacial environmental changes inferred from the molecular and compound-specific $\delta^{13}C$ analyses of sediments from Sacred Lake, Mt. Kenya. Geochimica et Cosmochimica Acta 63, 1383–1404.
Huang, Y., Dupont, L., Sarnthein, M., Hayes, J.M., Eglinton, G., 2000. Mapping of C_4 plant input from North West Africa into North East Atlantic sediments. Geochimica et Cosmochimica Acta 64, 3505–3513.
Huang, Y., Street-Perrott, F.A., Metcalfe, S.E., Brenner, M., Moreland, M., Freeman, K.H., 2001. Climate change as the dominant control on glacial–interglacial variations in C_3 and C_4 plant abundance. Science 293, 1647–1651.
Hughen, K., Eglinton, T., Xu, L., Makou, M., 2004. Abrupt tropical vegetation response to rapid climate changes. Science 304, 1955–1959.
Jacob, J., Huang, Y., Disnar, J.-R., Sifeddine, A., Boussafir, M., Albuquerque, A.L.S., Turcq, B., 2007. Paleohydrological changes during the last deglaciation in Northern Brazil. Quaternary Science Reviews 26, 1004–1015.
Jones, C.E., Halliday, A.N., Rea, D.K., Owen, R.M., 1994. Neodymium isotopic variations in North Pacific modern silicate sediment and the insignificance of detrital REE contributions to seawater. Earth and Planetary Science Letters 127, 55–66.
Jones, C.E., Halliday, A.N., Rea, D.K., Owen, R.M., 2000. Eolian inputs of lead to the North Pacific. Geochimica et Cosmochimica Acta 64, 1405–1416.
Kukla, G., Cilek, V., 1996. Plio-Pleistocene megacycles: record of climate and tectonics. Palaeogeography, Palaeoclimatology, Palaeoecology 120, 171–194.
Li, T., Philander, S.G.H., 1996. On the annual cycle of the eastern equatorial Pacific. Journal of Climate 9, 2986–2998.
Li, Q., Wang, P., Zhao, Q., Tian, J., Cheng, X., Jian, Z., Zhong, G., Chen, M., 2008. Paleoceanography of the mid-Pleistocene South China Sea. Quaternary Science Reviews 27, 1217–1233. doi:10.1016/j.quascirev.2008.02.007.
Lichtfouse, E., Derenne, S., Mariotti, A., Largeau, C., 1994. Possible algal origin of long chain odd *n*-alkanes in immature sediments as revealed by distributions and carbon isotope ratios. Organic Geochemistry 22, 1023–1027.
Lichtfouse, E., Eglinton, T., 1995. ^{13}C and ^{14}C evidence of pollution of a soil by fossil fuel and reconstruction of the composition of the pollutant. Organic Geochemistry 23, 969–973.
Lisiecki, E.L., Raymo, E.M., 2005. A Pliocene–Pleistocene stack of 57 globally distributed benthic $\delta^{18}O$ records. Paleoceanography 20, PA1003. doi:10.1029/2004PA001071.
Liu, Z., Herbert, T.D., 2004. High-latitude influence on the eastern equatorial Pacific climate in the early Pleistocene epoch. Nature 427, 720–723.
Luo, C., Mahowald, N.M., del Corral, J., 2003. Sensitivity study of meteorological parameters on mineral aerosol mobilization, transport, and distribution. Journal of Geophysical Research–Atmosphere 108, 4447. doi:10.1029/2203JD003483.
Lüthi, D., Le Floch, M., Bereiter, B., Blunier, T., Barnola, J.-M., Siegenthaler, U., Raynaud, D., Jouzel, J., Fischer, H., Kawamura, K., Stocker, T.F., 2008. High-resolution carbon dioxide concentration record 650,000–800,000 years before present. Nature 453. doi:10.1038/nature06949.
Marlowe, I.T., Brassell, S.C., Eglinton, G., Green, J.C., 1990. Long-chain alkenones and alkyl alkenoates and the fossil coccolith record of marine sediments. Chemical Geology 88, 349–375.
McGee, D., Marcantonio, F., Lynch-Stieglitz, J., 2007. Deglacial changes in dust flux in the eastern equatorial Pacific. Earth and Planetary Science Letters 257, 215–230.
Medina-Elizalde, M., Lea, D.W., 2005. The Mid-Pleistocene Transition in the tropical Pacific. Science 310, 1009–1012.
Mohtadi, M., Hebbeln, D., Nunez Ricardo, S., Lange, C.B., 2006. El Ninõ-like pattern in the Pacific during marine isotope stages (MIS) 13 and 11? Paleoceanography 21, PA1015. doi:10.1029/2005PA001190.
Mora, G., Pratt, L.M., 2002. Carbon isotopic evidence from paleosols for mixed C_3/C_4 vegetation in the Bogota Basin, Colombia. Quaternary Science Reviews 21, 985–995.
Mudelsee, M., Schulz, M., 1997. The Mid-Pleistocene climate transition: onset of 100 ka cycle lags ice volume build-up by 280 ka. Earth and Planetary Science Letters 151, 117–123.
Ohkouchi, N., Kawamura, K., Kawahata, H., Taira, A., 1997. Latitudinal distributions of terrestrial biomarkers in the sediments from the Central Pacific. Geochimica et Cosmochimica Acta 61, 1911–1918.
Poynter, J.G., Farrimond, P., Robinson, N., Eglinton, G., 1989. Aeolian-derived higher plant lipids in the marine sedimentary record: links with palaeoclimate, in Paleoclimatology and Paleometeorology. In: Leine, M., Sarnthein, M. (Eds.), Modern and Past Patterns of Global Atmospheric Transport. Kluwer Academic Publishers, Norwell, pp. 435–462.
Prahl, F.G., Mix, A.C., Sparrow, M.A., 2006. Alkenone paleothermometry: biological lessons from marine sediment records off western South America. Geochimica et Cosmochimica Acta 70, 101–117.
Prospero, J.M., Bonatti, E., 1969. Continental dust in the atmosphere of the eastern equatorial Pacific. Journal of Geophysical Research 74, 3362–3371.
Raymo, M.E., Oppo, D.W., Curry, W.B., 1997. The mid-Pleistocene climate transition: a deep sea carbon isotopic perspective. Paleoceanography 12, 546–559.
Rommerskirchen, F., Eglinton, G., Dupont, L., Guntner, U., Wenzel, C., Rullkotter, J., 2003. A north to south transect of Holocene southeast Atlantic continental margin sediments: relationship between aerosol transport and compound-specific $\delta^{13}C$ land plant biomarker and pollen records. Geochemistry, Geophysics, Geosystems 4 (12), 1101. doi:10.1029/2003GC000541.
Rommerskirchen, F., Eglinton, G., Dupont, L., Rullkotter, J., 2006. Glacial/interglacial changes in southern Africa: compound-specific $\delta^{13}C$ land plant biomarker and pollen records from southeast Atlantic continental margin sediments. Geochemistry, Geophysics, Geosystems 7, Q08010. doi:10.1029/2005GC001223.
Schefu, E., Schouten, S., Fred Jansen, J.H., Sinninghe Damsté, J.S., 2003a. African vegetation controlled by tropical sea surface temperatures in the mid-Pleistocene period. Nature 422, 418–421.
Schefu, E., Ratmeyer, V., Stuut, J.-B.W., Jansen, J.H.F., Sinninghe Damsté, J.S., 2003b. Carbon isotope analyses of *n*-alkanes in dust from the lower atmosphere over the central eastern Atlantic. Geochimica et Cosmochimica Acta 67, 1757–1767.
Schefu, E., Sinninghe Damsté, J.S., Jansen, J.H.F., 2004. Forcing of tropical Atlantic sea surface temperatures during the mid-Pleistocene transition. Paleoceanography 19, PA4029. doi:10.1029/2003PA000892.
Shackleton, N.J., Berger, A., Peltier, W.R., 1990. An alternative astronomical calibration of the lower Pleistocene timescale based on ODP Site 677. Transactions of the Royal Society of Edinburgh, Earth Sciences 81, 251–261.
Shyu, J.-P., Chen, M.-P., Shieh, Y.-T., Huang, C.-K., 2001. A Pleistocene paleoceanographic record from the north slope of the Spratly Islands, southern South China Sea. Marine Micropaleontology 42, 61–93.
Shepherd, T., Griffiths, D.W., 2006. The effects of stress on plant cuticular waxes. New Phytologist 171, 469–499. doi:10.1111/j.1469-8137.2006.01826.x.
Simoneit, B.R.T., 1984. Organic matter of the troposphere: III. Characterization and sources of petroleum and pyrogenic residues in aerosols over the western United States. Atmospheric Environment 18, 51–67.
Srinivasan, J., Smith, G., 1996. Meridional migration of tropical convergence zones. Journal of Climate 9, 1189–1202.
Standley, L.J., Simoneit, B.R.T., 1987. Composition of extractable organic matter in smoke particles from prescribed burns. Environmental Science and Technology 21, 163–169.
Still, C.J., Berry, J.A., Collatz, G.J., DeFries, R.S., 2003. Global distribution of C_3 and C_4 vegetation: carbon cycle implications. Global Biogeochemical Cycles 17, 1006. doi:10.1029/2001GB001807.
Street-Perrott, F.A., Huang, Y., Perrott, R.A., Eglinton, G., Barker, P., Khelifa, L.B., Harkness, D.D., Olago, D.O., 1997. Impact of lower atmospheric carbon dioxide on tropical mountain ecosystems. Science 278, 1422–1426.
Suganuma, Y., Yamazaki, T., Kanamatsu, T., 2009. South Asian monsoon variability during the past 800 kyr revealed by rock magnetic proxies. Quaternary Science Reviews 28, 926–938.
Sun, Y., Chen, J., Clemens, S.C., Liu, Q., Ji, J., Tada, R., 2006. East Asian monsoon variability over the last seven glacial cycles recorded by a loess sequence from the northwestern Chinese Loess Plateau. Geochemistry, Geophysics, Geosystems 7, Q12Q02. doi:10.1029/2006GC001287.
Ternois, Y., Sicre, M.-A., Boireau, A., Beaufort, L., Miquel, J.-C., Jeandel, C., 1998. Hydrocarbons, sterols and alkenones in sinking particles in the Indian Ocean sector of the Southern Ocean. Organic Geochemistry 28, 489–501.
Thompson, L.G., Thompson, E.M., Henderson, K.A., 2000. Ice-core palaeoclimate records in tropical South America since the Last Glacial Maximum. Journal of Quaternary Science 15, 377–394.

Timmermann, A., Lorenz, S.J., An, S.-I., Clement, A., Xie, S.-P., 2007. The effect of orbital forcing on the mean climate and variability of the tropical Pacific. Journal of Climate 20, 4147–4159.

Tulloch, A.P., 1976. Chemistry of waxes of higher plants. In: Kolattukudy, P.E. (Ed.), Chemistry and Biochemistry of Natural Waxes. Elsevier, Amsterdam, pp. 235–287.

Vogts, A., Moossen, H., Rommerskirchen, F., Rullktter, J.r., 2009. Distribution patterns and stable carbon isotopic composition of alkanes and alkan-1-ols from plant waxes of African rain forest and savanna C_3 species. Organic Geochemistry 40, 1037–1054.

Wang, X., Auler, A.S., Edwards, R.L., Cheng, H., Cristalli, P.S., Smart, P.L., Richards, D.A., Shen, C.-C., 2004. Wet periods in northeastern Brazil over the past 210 kyr linked to distant climate anomalies. Nature 432, 740–743.

Wang, X., Auler, A.S., Edwards, R.L., Cheng, H., Ito, E., Wang, Y., Kong, X., Solheid, M., 2007. Millennial-scale precipitation changes in southern Brazil over the past 90,000 years. Geophysical Research Letters 34, L23701. doi:10.1029/2007GL031149.

Yamamoto, M., Yamamuro, M., Tada, R., 2000. Late Quaternary records of organic carbon, calcium carbonate and biomarkers from Site 1016 off Point Conception, California margin. Proceedings ODP, Scientific Results 167, 183–194.

Zender, C.S., Bian, H.S., Newman, D., 2003. Mineral Dust Entrainment and Deposition (DEAD) model: description and 1990s dust climatology. Journal of Geophysical Research 108 (D14), 4416. doi:10.1029/2002JD002775.

Zhang, Z., Zhao, M., Lu, H., Faiia, A.M., 2003. Lower temperature as the main cause of C_4 plant declines during the glacial periods on the Chinese Loess Plateau. Earth and Planetary Science Letters 214, 467–481. doi:10.1016/S0012-821X(03)00387-X.